Accurate characterization of intermodulation noise in multi carrier wide band power amplifiers based on a digital synthesis of pseudo noise gaussian stimuli

T. Reveyrand, D. Barataud, J-M. Nébus, A. Mallet, F. Gizard, L. Lapierre, J. Sombrin

Published in
Annals of telecommunications, Vol. 61, No 5-6, pp.627-644,
May / June 2006

Accurate characterization of intermodulation noise in multi carrier wide band power amplifiers based on a digital synthesis of pseudo noise gaussian stimuli

T Reveyrand* , D Barataud* , JM Nebus* , A Mallet** , F Gizard** , L Lapierre**J Sombrin **

***Abstract*—This paper presents an accurate technique for the characterization of intermodulation noise in wide band multi carrier power amplifiers. Band limited pseudo noise stimuli which are generated by using a computer controlled arbitrary waveform generator (AWG) connected to an I/Q modulator drive the input of the amplifier under test (AUT). The complex envelopes of the pseudo noises are measured using a sampling scope. A vector error correction is applied in order to remove systematic errors due to the imperfections of the measurement channels .Using this technique, the linearity of L and Ka band amplifiers was characterized by the noise power ratio criterion (NPR). This paper focuses also on the particular attention that must be paid to the statistical properties and peak to average ratio (PAR) of pseudo noise test signals which significantly impact the NPR measurement accuracy.**

***Key words*—"Noise Power Ratio" measurements, time-domain envelope measurements, nonlinear amplifier characterization.**

Caractérisation précise du bruit d'inter modulation dans les amplificateurs de puissance large bande et multiporteuse fondée sur la synthèse numérique de pseudo bruits gaussiens

T Reveyrand* , D Barataud* , JM Nebus* , A Mallet** , F Gizard** , L Lapierre**J Sombrin **

***Résumé* – Ce papier présente une technique précise de caractérisation du bruit d'intermodulation dans les amplificateurs de puissance large bande et multiporteuse. Des pseudo bruits a bande limitée qui sont générés par un générateur de fonctions arbitraire connecté a un modulateur I/Q excitent l'entrée de l'amplificateur sous test. Les enveloppes complexes des pseudo bruits sont mesurées en utilisant un oscilloscope à échantillonnage. Une correction vectorielle est appliquée pour enlever les erreurs systématiques dues aux imperfections des canaux de mesure. En utilisant cette technique la linéarité d'amplificateurs en bande L et Ka a été caractérisée en terme de rapport de puissance de bruit. Cet article se focalise aussi sur l'attention particulière qui doit être portée aux propriétés statistiques et au rapport puissance crête à puissance moyenne des signaux de pseudo bruit qui ont un impact significatif sur la précision des mesures de rapport de puissance de bruit.**

***Mots clés* —Mesures de rapport de puissance de bruit, mesures d'enveloppe temporelle, caractérisation d'amplificateur non linéaire.**

* IRCOM, CNRS UMR 6615, University of Limoges, 87000 Limoges, France.
** CNES French space agency 31401 Toulouse, France.

I. INTRODUCTION

Many existing and future communication systems such as satellite payloads, base stations for mobile communications or indoor communications require multicarrier operation of power amplifiers [1]. [2].
Multicarrier signals are non envelope constant signals with large peak to average power ratios (in the order of 10 dB). The power amplification of such signals is well known to be critical in terms of power efficiency versus linearity [3].
As a consequence the linearity of power amplifiers cannot be accurately characterized using classical 2 tone measurements The statistical properties of multicarrier modulated signals can be quite different. Those used in digital satellite communications can be considered very similar to those of Gaussian band limited processes. Thus, band limited noise is a quite convenient test signal for the linearity characterization of power amplifiers. The ratio between the useful signal power and the intermodulation noise power (namely the NPR) in the output signal spectrum of power amplifiers represents a very useful figure of merit for link budget and BER calculations.
The conventional NPR characterization technique consists in loading the power amplifier input with a band limited white Gaussian noise by using an analog noise source. A narrow noise free window called a notch in the input noise spectrum enables to probe the intermodulation noise generated in the output signal spectrum [4] [5] by using a spectrum analyzer.
Such a method suffers from a lack of flexibility. The modification of the notch bandwidth or frequency position is not very straightforward and requires a set of physical notch filters. On the contrary, we will see that by using the method proposed in this paper it is quite easy to create a notch by simply setting to zero a subset of spectral lines of a digitally synthesized pseudo noise.
Another drawback of the analog noise source method is that comparisons between measurements and harmonic balance simulations which are often wished in a circuit design process are not quite traceable. Moreover the improvement of measurement accuracy using calibration procedures similar to those achieved for vector network analyzer is somewhat questionable. In fact, when using the analog noise source method, the calibration steps consist only in the determination of power level offsets between the reference planes of the amplifier under test and the measurement planes. On the contrary more sophisticated vector calibration methods including frequency dependent error terms can be implemented if the noise measurement principle is based on the digital generation of an appropriate set of spectral lines as it is proposed in this paper.

II. DIGITALLY SYNTHESIZED PSEUDO NOISE CONDITIONING

A. NPR stimulus generation

For the characterization of intermodulation noise generated by non linear power amplifiers, let us consider the input and the output signals as:

$$x(t) = A(t)\cos\left[\omega_0 t + \varphi(t)\right] \tag{1a}$$

$$y(t) = B(t)\cos\left[\omega_0 t + \theta(t)\right] \tag{1b}$$

The associated base band complex envelopes referenced to the center frequency f_0 of the amplifier bandwidth are:

$$X(t) = A(t)e^{j\varphi(t)} \tag{2a}$$

$$Y(t) = B(t)e^{j\theta(t)} \tag{2b}$$

Out of band spectral components (harmonics and low frequency beats created by nonlinearities) are not considered here in the response *Y(t)*.
It does not mean that these out of band signals that exist within the amplifier under test do not have an impact on the useful in band output signal Y(t). They do and they contribute to the non-quasi-static nonlinear behavior of the amplifier. For our purpose here, they are only assumed to be filtered at the output RF port by RF matching circuits. X(t) describes the information to be transmitted. Y(t) includes both the amplified useful signal and the intermodulation noise.
The characteristics of X(t) require a very accurate knowledge and a careful attention in order to clearly define and discuss the intermodulation noise shape obtained and the associated linearity criterion used (NPR in the present paper).
The four main characteristics of X(t) that strongly impact the nonlinear behavior of the AUT (Amplifier Under Test) are:

- the average power,
- the peak to average power ratio (PAR),
- the probability density function (pdf) and the frequency bandwidth.

Indeed, two input signals with the same average power and the same frequency bandwidth but different PARs will set the AUT into two significantly different nonlinear behaviors thus leading to different intermodulation noise shapes.
In the same manner, two input signals with the same average power and PAR but different pdfs lead also to different intermodulation noise shapes.
We consider in this paper X(t) as a Gaussian band limited process which is representative of multi carrier signals encountered in real applications. According to the central limit theorem, X(t) can be represented by the sum of a sufficient number of non correlated CW tones as expressed in (3) and sketched in figures 1 .

$$X(t) = \sum_{n=-N/2}^{N/2} A.e^{j(n\Delta\omega t+\varphi_n)} \tag{3}$$

φ_n is a random phase draw. Its pdf is uniform on [0; 2π].

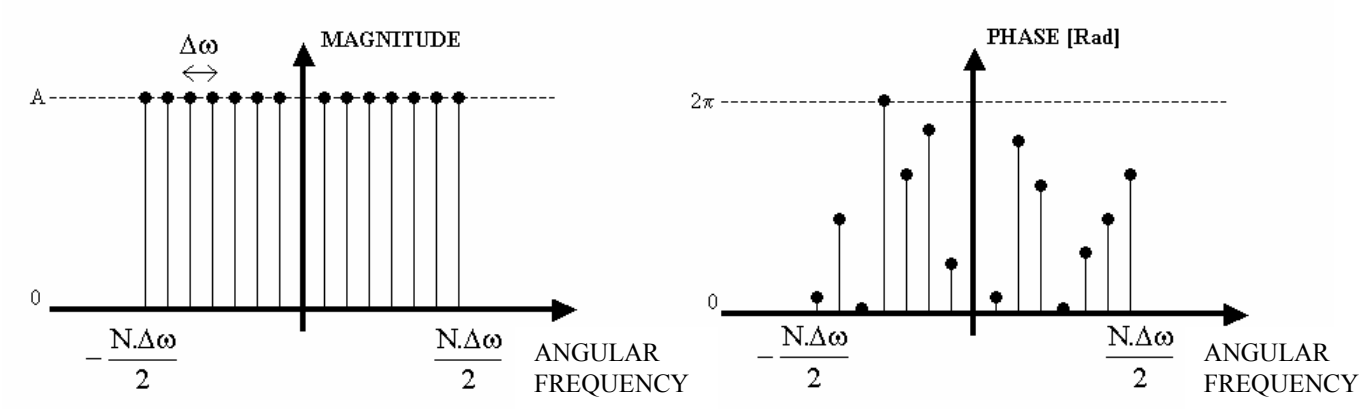

Fig. 1: Spectrum of X(t).
Spectre de X(t).

If the number N of the discrete spectral lines is large enough, the time domain waveform and the statistical properties of X(t) are not sensitive to the random phase draw φ_n. Spectral lines at $n\Delta\omega$, covering the $N\Delta\omega$ frequency bandwidth must be non correlated. Otherwise, both magnitude and phase modulations are not representative of gaussian stimuli. For example, if the negative spectral lines of X(t) are the complex conjugates of the positive spectral lines [6], a purely real envelope is obtained. It corresponds to a strong correlation case and the signal has a 2 dB higher PAR compared to the non correlated case. Such a stimulus would drive an Amplifier Under Test (AUT) into a nonlinear operation mode which is non compliant with real encountered satellite applications. As a consequence, NPR characterisation using such a stimulus would be pessimistic [7].
These main remarks are illustrated in the figures 2 and 3.
Figure 3 gives a representation of a pseudo noise with non correlated spectral lines in the complex I/Q plane. Gaussian shapes of pdfs for both real and imaginary parts are also represented.

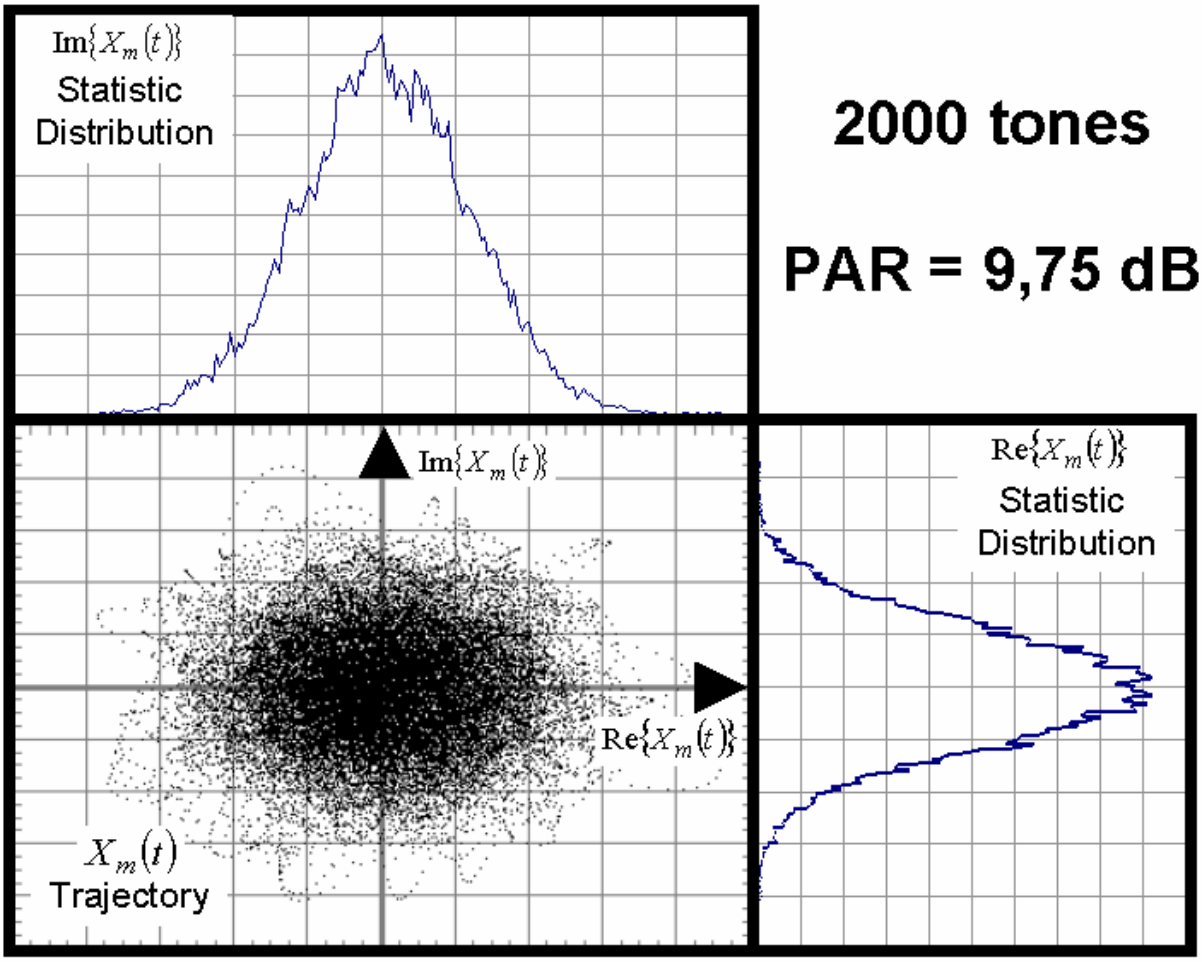

Fig. 2: Trajectory and pdf of $X_m(t)$ for a given phase draw. Spectral side bands of the signal are non-correlated.
Trajectoire dans le plan complexe et densité de probabilité de $X_m(t)$ pour un tirage de phase donné. Les bandes latérales du spectre du signal ne sont pas corrélées

In figure 3, the PAR versus the number of tones is plotted for both cases (correlated and non correlated). For each case an area is defined because, for each number of tones, 50 different phase draws are taken into account. This figure illustrates that for the correlated case the PAR is about 2 dB higher than for the non correlated case .

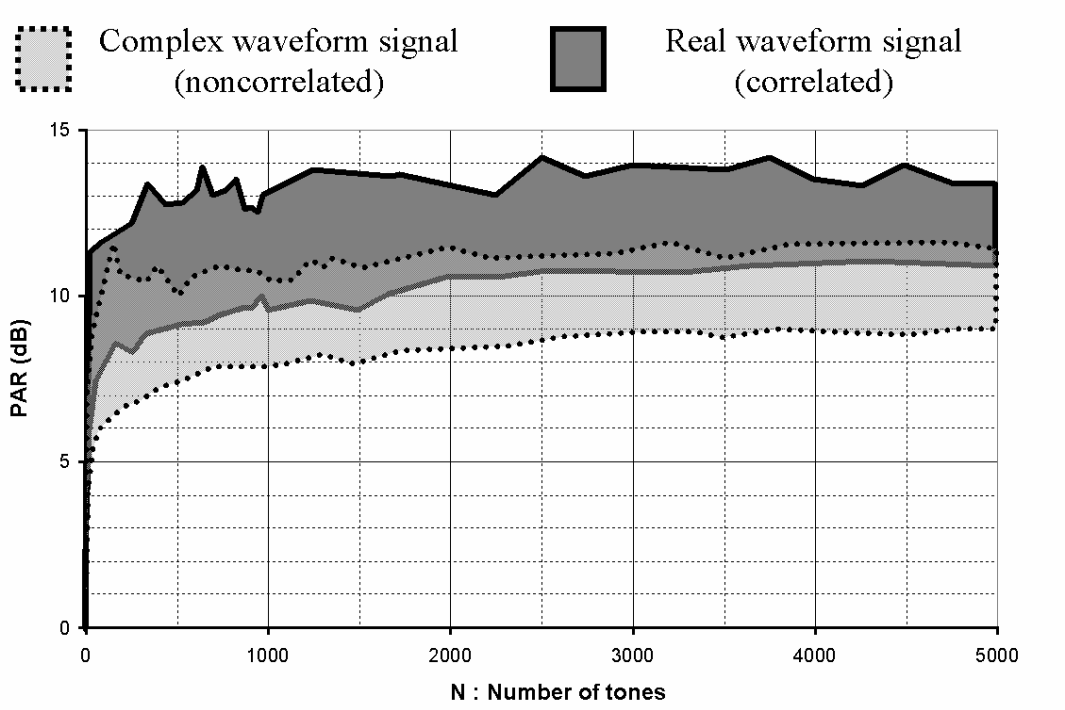

Fig. 3: Peak to Average Ratio of X(t) obtained for 50 different phase draws versus the number of tones (correlated spectrum or not).
Rapport de puissance crête à moyenne de X(t) obtenue pour 50 tirages de phase différents en fonction du nombre de porteuses (spectre à bandes latérales corrélées ou non)

The instantaneous power of a real Gaussian signal obeys a gamma probability density law given by:

$$\Gamma\left(\frac{1}{2}\ ,\ \frac{1}{2}\right) = \frac{1}{2\sqrt{\pi}} \times e^{-\frac{x}{2}} \times \left(\frac{x}{2}\right)^{-\frac{1}{2}} \tag{4}$$

This law has an average of 1 and a standard deviation equal to $\sqrt{2}$.
The instantaneous power of a complex Gaussian signal obeys a gamma probability density law given by:

$$\Gamma(1\ ,\ 1) = e^{-x} \tag{5}$$

This law is also called an exponential law. It has an average of 1 and a standard deviation of 1.

The probability for a real signal to exceed a given PAR is higher than it is for a complex signal. At a given probability of 1.E-03, the real signal PAR is 2 dB higher than the complex signal one (figure 4).

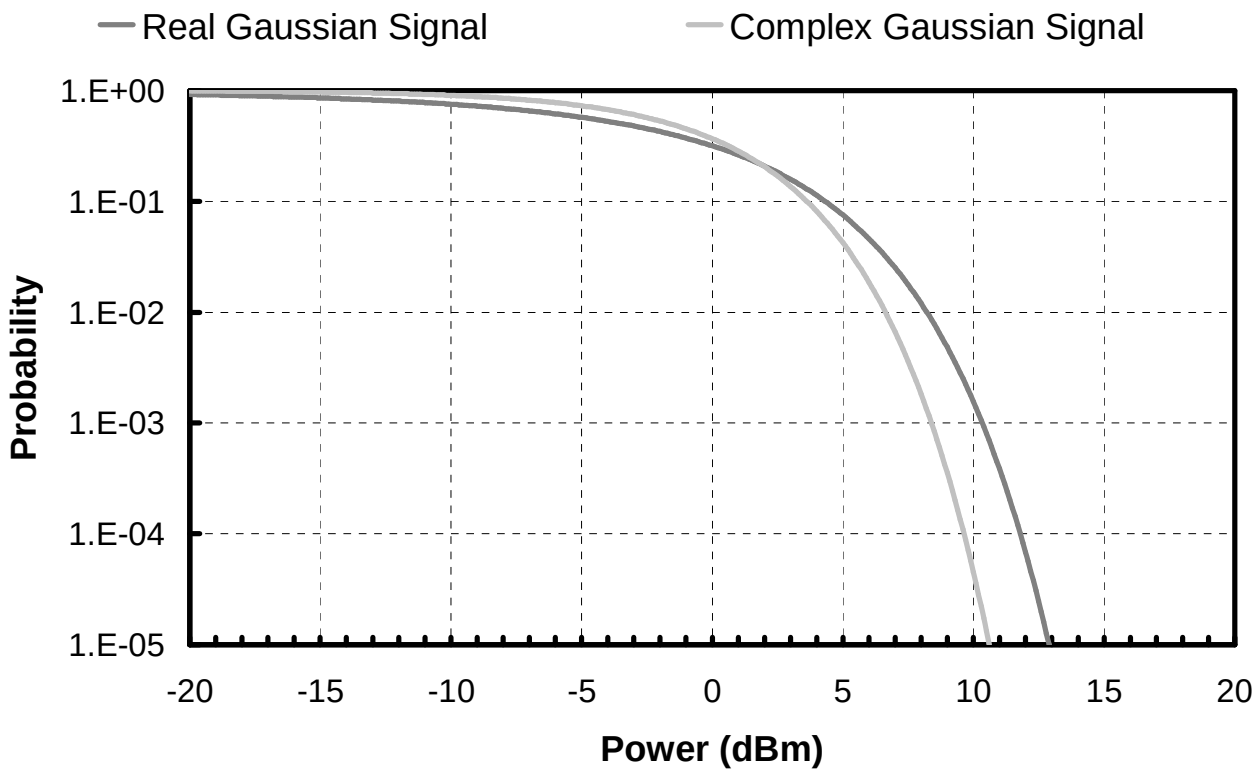

Fig. 4: Probability for a signal to exceed a given instantaneous power. The average power of both the real and complex signals is 0 dBm.
Probabilité pour le signal de dépasser une puissance instantanée donnée. La puissance moyenne pour les signaux réel et complexe est de 0 dBm

A slightly modified spectrum of X(t) must be created in order to probe the intermodulation noise exhibited by the nonlinear operation of power amplifiers. For that, a few tones are rejected to create a notch. This leads to a modified test signal $X_m(t)$ as illustrated in figure 5.

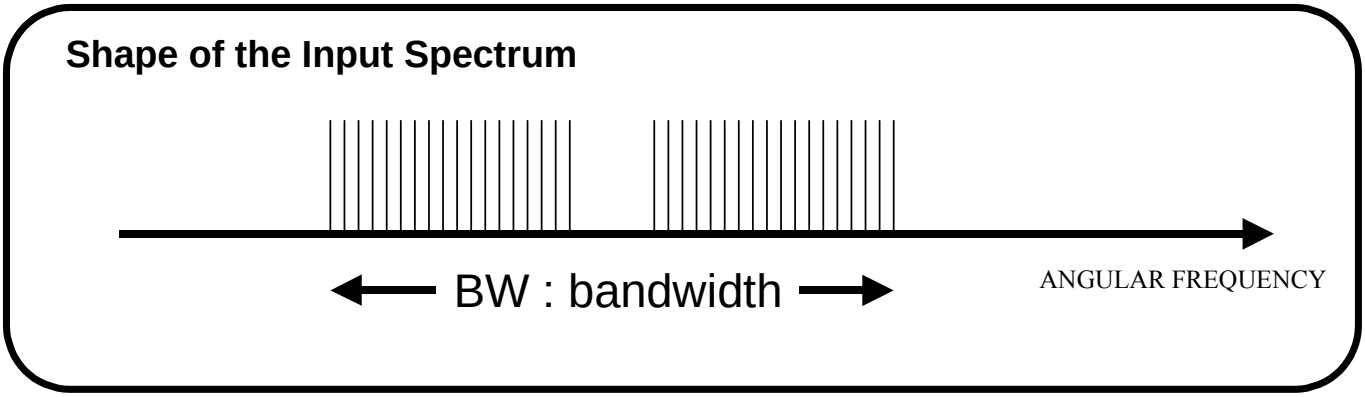

Fig. 5: $X_m(t)$ spectrum : the stimulus which drives an amplifier under test for NPR characterization.
Spectre de $X_m(t)$, le signal qui excite un amplificateur sous test pour la caractérisation de rapport de puissance de bruit

Basically, when such a signal spectrum drives the input of a nonlinear device, the shape of the output signal spectrum is shown in the figure 6.
$\overline{P}_{signal}$ is the average power of the (N-M) signal lines; $\overline{P}_{noise}$ is the average power of the M intermodulation lines.

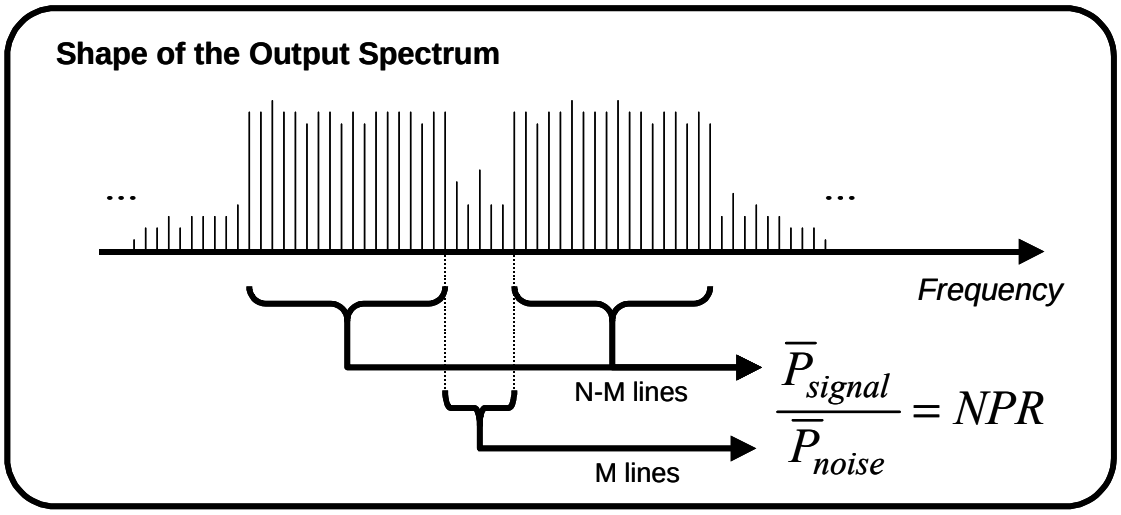

Fig. 6: Output spectrum of an amplifier under test during a NPR characterization.
Spectre de sortie d'un amplificateur sous test lors d'une caractérisation en rapport de puissance de bruit.

We define the Noise Power Ratio (NPR) by:

$$NPR_{dB} = 10 \times \log_{10}\left(\frac{\overline{P}_{\text{signal}}}{\overline{P}_{\text{noise}}}\right) \tag{6}$$

B. Theoretical NPR variance

Specific cautions must be taken in order to get an accurate NPR characterisation.
First, the notch must be in the order or less than 5% of the total bandwidth BW, so that the time domain waveform and the pdf of X(t) and $X_m(t)$ remain the same and very close to those of a band limited gaussian process. Consequently, a nonlinear device driven by X(t) or $X_m(t)$ will exhibit the same intermodulation noise shape. Otherwise, the accuracy and the validity of NPR measurement results are affected.
Secondly, the shape of the output spectral lines within the notch as well as out of the notch depends on the phase draw φ_n. So, NPR value obtained by this technique is a random variable whose variance must be minimized.

As far as the number of tones (N-M) is large enough, the variance of the average power of the spectral lines out of the notch is very low. Furthermore this average power, which includes both the power of the useful test signal and a part of the intermodulation noise generated by the non linearity, is very close to the average power of the useful test signal $(\overline{P}_{signal})$ for NPR values higher than 15 dB.

However, the variance of the mean power of the M intermodulation lines within the notch $(\overline{P}_{noise})$ is not negligible and must be analyzed. It can be assumed that the power Pi of each intermodulation line taken separately follows a same, but a priori unknown pdf with a mean value m and a variance $\sigma 2$. Applying the central limit theorem, the average power of the sum of the M intermodulation lines converges on a gaussian

distribution. Equation 7 gives the centered and reduced expression for the average power of the intermodulation noise.

$$\bar{P}_{\text{noise}}^{\text{reduced}} = \frac{1}{\sqrt{M}}\left[\frac{M\bar{P}_{\text{noise}} - mM}{\sigma}\right] = \sqrt{M}\left[\frac{\bar{P}_{\text{noise}} - m}{\sigma}\right] \quad \text{where M is the number of tones within the notch.} \quad (7)$$

$\bar{P}_{\text{noise}}^{\text{reduced}}$ is simply a random variable corresponding to the total noise power within the notch. This random variable is centered (mean value equal to zero) and reduced (σ=1). It is only used to evaluate and plot the NPR error (ΔNPR) obtained by using digital pseudo noise stimuli instead of real analog noise stimuli.
Consequently, the NPR error is linked to the average power calculated with the intermodulation spectral lines within the notch and can be simplified to the following expression:

$$\Delta NPR \approx 10 \times \log_{10}\left[\left(\frac{\sigma}{m}\right) \times \left(\frac{\bar{P}_{\text{noise}}^{\text{reduced}}}{\sqrt{\text{M}}}\right) + 1\right] \quad (8)$$

Measurements have shown a value of m/σ ratio in the order of 0.75 [8] in agreement with a theoretical value of 1 [9]. Thus, the NPR error (ΔNPR) at 2σ versus the number of intermodulation tones into the notch (M) can be sketched in figure 7.

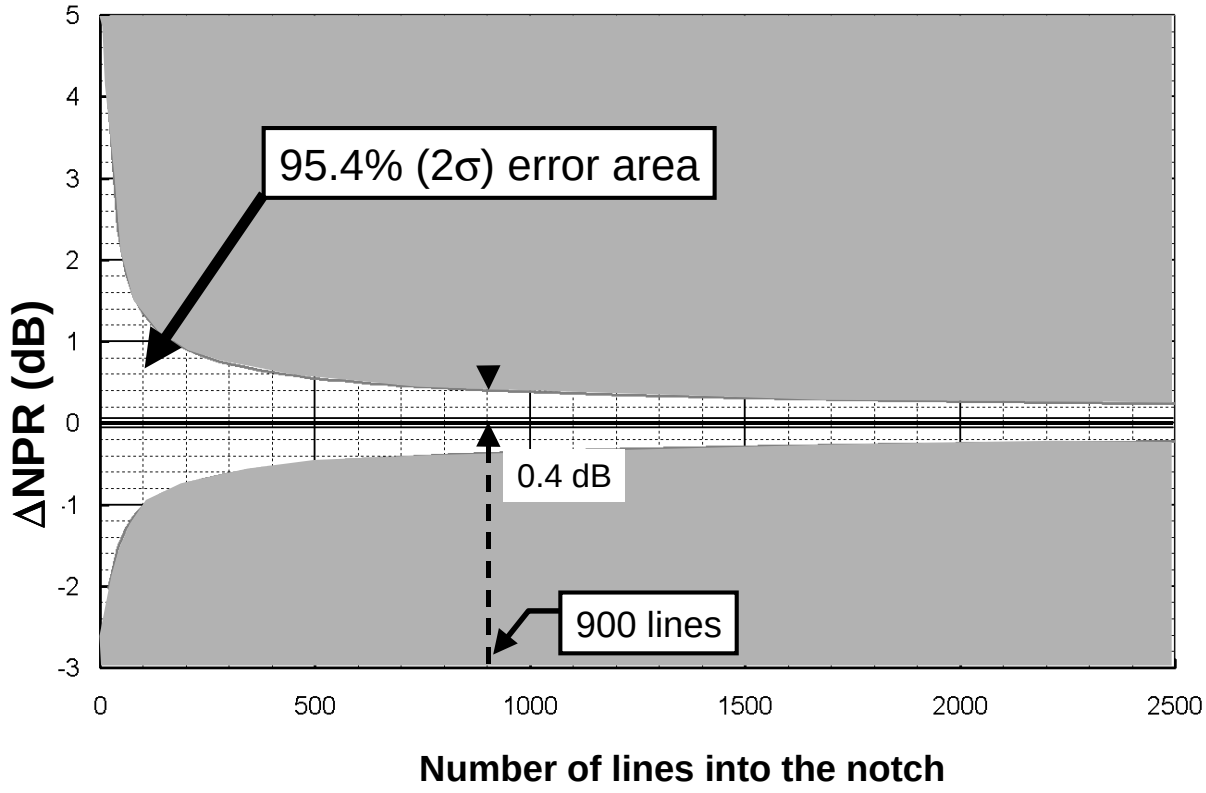

Fig. 7: NPR error at 2σ (i.e. 95.4%) versus the number of intermodulation tones into the notch (M).
Erreur de NPR à 2σ en fonction du nombre de raies d'inter modulation dans le trou

For example, a NPR error lower than 0.4 dB in 95.4% of measurements can be obtained with 900 intermodulation lines in the notch.
As a conclusion, there are two ways to get accurate NPR measurements using the proposed discrete spectrum approach. For example, if we need a 0.4 dB accuracy for 95.4% of measurements, either we can do only one measurement with a fixed phase draw $\{\varphi_n\}$ and a 18000 tone signals: in this case, 900

intermodulation tones will be present in a 5% notch; or we do several measurements with different phase draws and a limited number of tones (i.e. 900 tones with 20 different phase draws).
In this second case NPR measurement results have to be averaged.

III. MEASUREMENT SETUP AND CALIBRATION PROCEDURE

A. Measurement setup at L and S band [10]

A block diagram is sketched in figure 8. The signal generation part (transmitter part) consists of a computer controlled arbitrary waveform generator (two channels, 12 bits, 250 MHz sampling rate), a I/Q modulator for frequency up conversion, a band pass filter for image rejection and a very linear amplifier that provides sufficient power to set the AUT into a nonlinear regime. A step attenuator is used to perform a power sweep during measurements in order to record the NPR versus input power.
The measurement channel part (receiver part) consists of a I/Q demodulator and a sampling scope (8 bits, 500 MHz bandwidth, 1 GHz sampling rate). A calibrated step attenuator is used to keep the demodulator operating in its linear region.

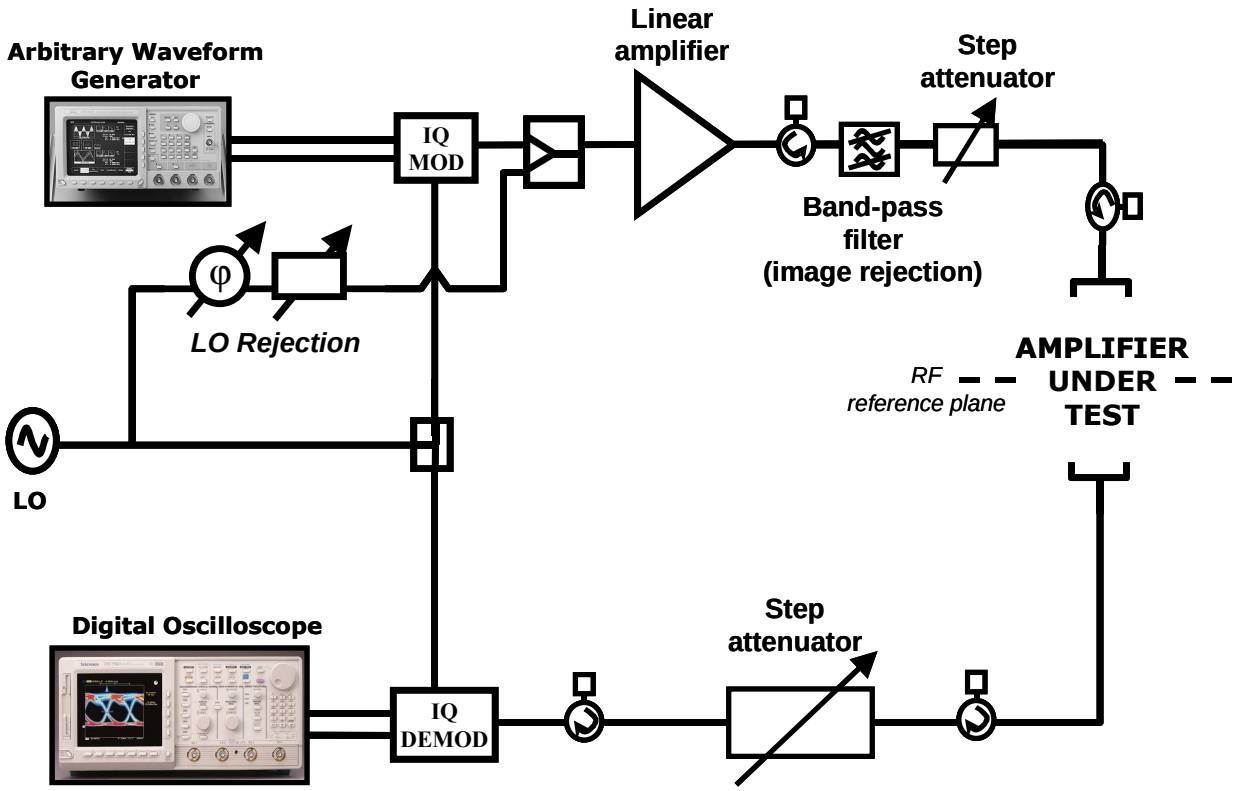

Fig. 8: Measurement setup block diagram.
Synoptique du banc de mesure

A FFT of the measured time domain signals I(t) and Q(t) is performed for NPR extraction.
Band pass instead of low pass pseudo noise stimuli are in fact synthesized using the AWG. A low frequency noise spectrum centered around a 40 MHz IF frequency is generated. The 2 AWG channels enable to generate both real and imaginary parts of the complex envelope $X_{IF}(t)$ which drives the IQ modulator :

$$X_{IF}(t) = \sum_{n=1}^{\frac{N}{2}-\frac{M}{2}} A e^{j(\omega_n t+\varphi_n)} + \sum_{n=\frac{N}{2}+\frac{M}{2}}^{N} A e^{j(\omega_n t+\varphi_n)} \quad (9)$$

M is the number of rejected tones, and N is in the order of a few thousands.
A few tones are ideally removed from the spectrum around IF (figure 9).

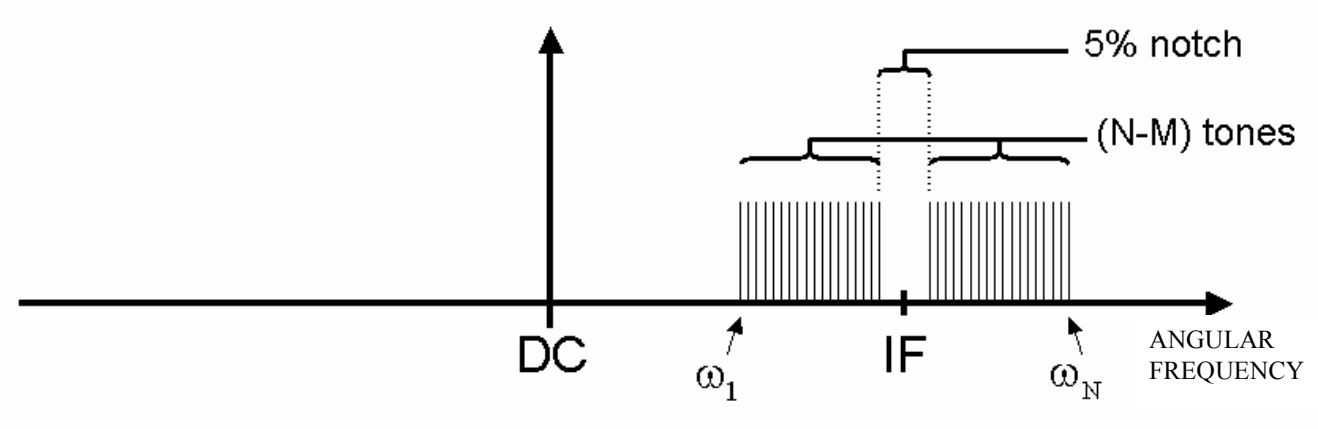

Fig. 9: Spectrum of $X_{IF}(t)$
Spectre de $X_{IF}(t)$

A tunable band pass filter enables an easier image and LO spurious rejections at the output of the frequency up conversion.

B. Calibration procedure

The receiver part of the measurement system needs to be calibrated to remove systematic vector errors. For that purpose, a CW microwave source is connected at the RF reference plane and a power meter is used as shown in figure 10.

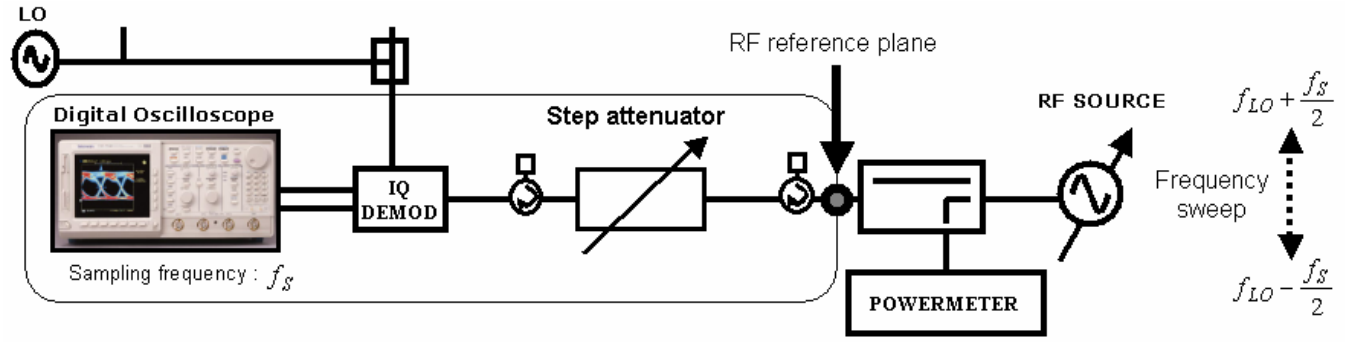

Fig. 10: Calibration procedure of the receiver part
Procédure de calibrage de la partie réceptrice

The frequency of the microwave source is swept each side away from the local oscillator frequency scanning a large frequency range (5ΔF) compared to the noise bandwidth (ΔF) that will be used during NPR characterization. The magnitude of the CW signal supplied by the source is measured by the power meter and by the two channels of the scope recording the associated IF sine waves I(t) and Q(t) .IF corresponds here to the difference between the fixed local oscillator frequency and the microwave source frequency.
The ratio between the power meter measurements and the magnitude of the waves recorded by the scope provides the conversion losses KI and KQ of the in phase and in quadrature paths of the I/Q demodulator. The phase imbalance Δϕ of the demodulator is also determined from the scope measurements.
Figures 11 and 12 show conversion losses KI and KQ and the phase imbalance Δϕ versus the frequency offset each side away from the local oscillator frequency .The sampling frequency of the scope was fixed to

500 MHz.

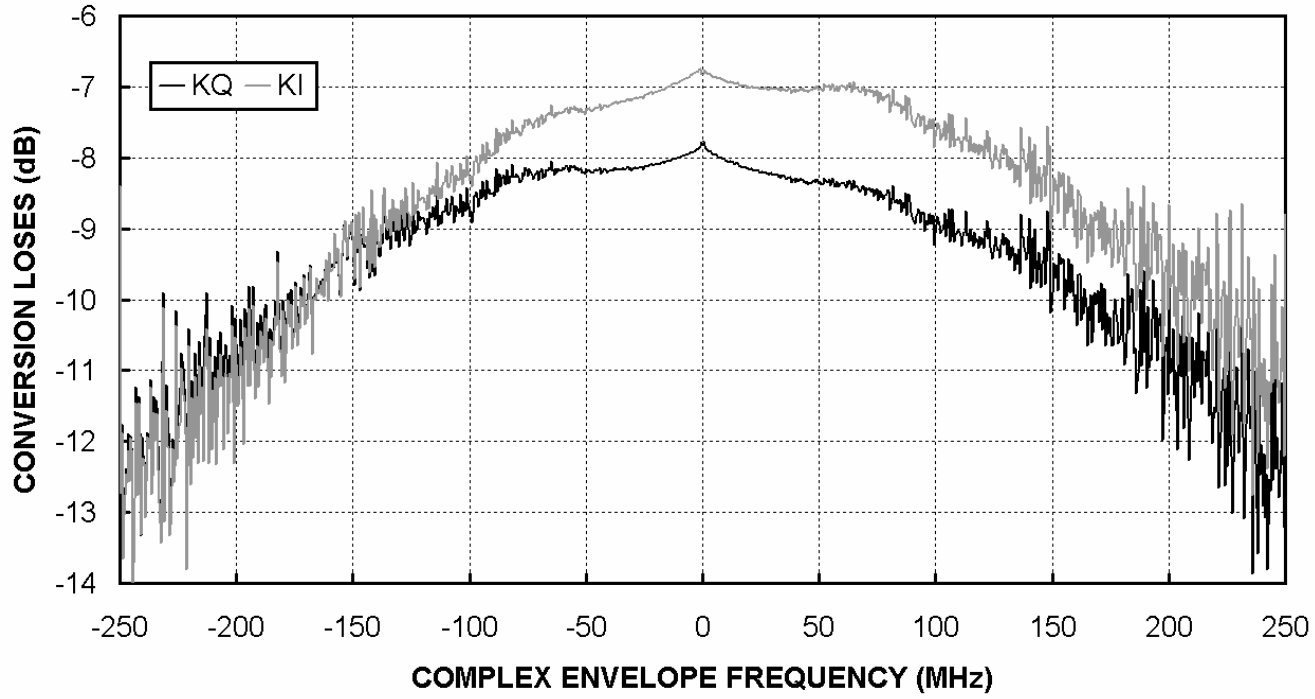

Fig. 11: Conversion losses (KQ and KI) versus envelope frequency (fLO=1.535 GHz; 16 dBm)
Pertes de conversion KQ et KI en fonction de la fréquence d'enveloppe (fLO=1.535 GHz; 16 dBm)

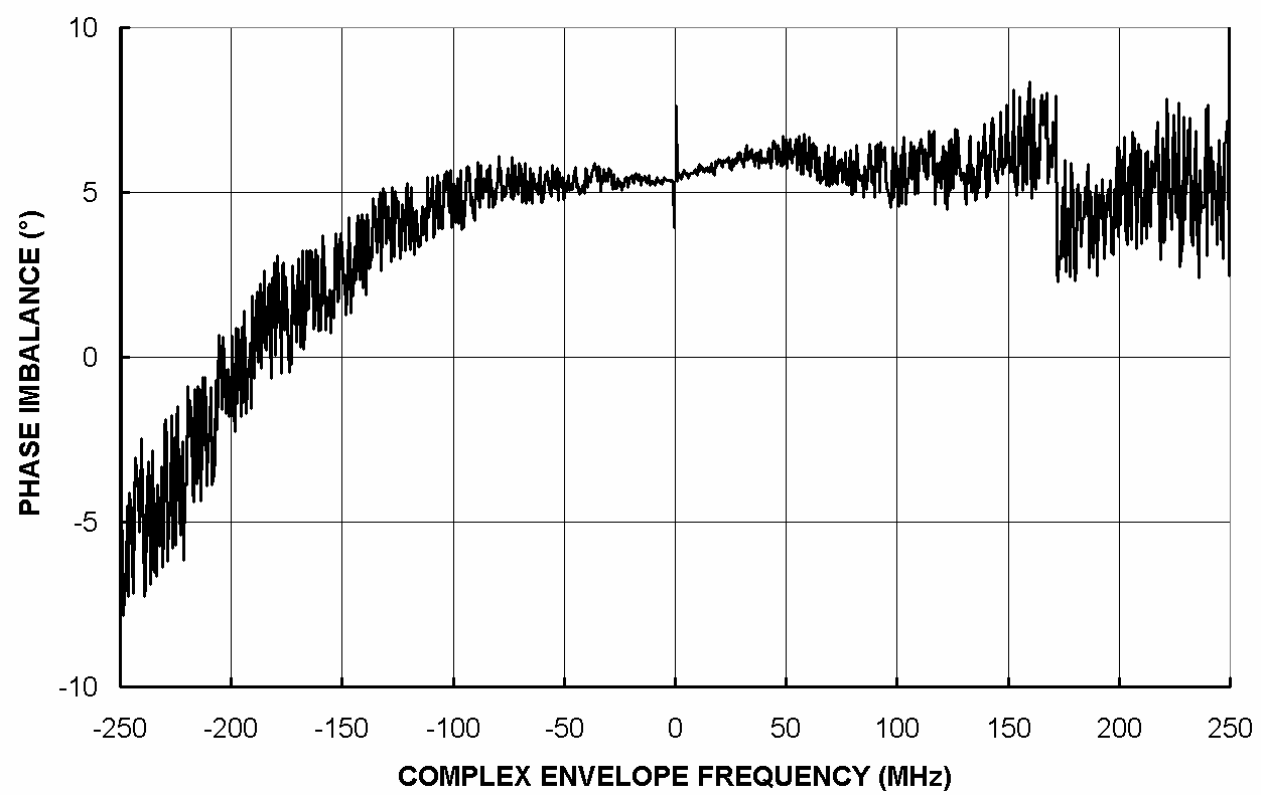

Fig. 12: Phase imbalance $\Delta\phi$ versus envelope frequency (f_{LO}=1.535 GHz; 16 dBm)
Déséquilibre de phase $\Delta\phi$ en fonction de la fréquence d'enveloppe (f_{LO}=1.535 GHz; 16 dBm)

We have checked that the group delay of the in phase path of the demodulator remains constant on the frequency bandwidth of interest by measuring it with a vector network analyzer configured for mixer measurements.

Using now these calibration parameters (KI, KQ and Δϕ), we correct the measured low frequency spectral lines in the frequency domain :

$$X_{RF\ ref\_plane}(t) = \left\{ FFT^{-1}\left[\frac{I(f)}{K_I(f)} \right] \right\} + j \left\{ FFT^{-1}\left[\frac{Q(f)}{K_Q(f) \times e^{j\Delta\varphi(f)}} \right] \right\} \quad (10)$$

IV. Measurement results of a L band SSPA

Figure 13 presents RF spectrum measurements at the input and the output of a 24 dBm TI-HFET amplifier at 2,11 GHz.

A 20 MHz noise bandwidth (9500 tones) with a 5% notch was applied.

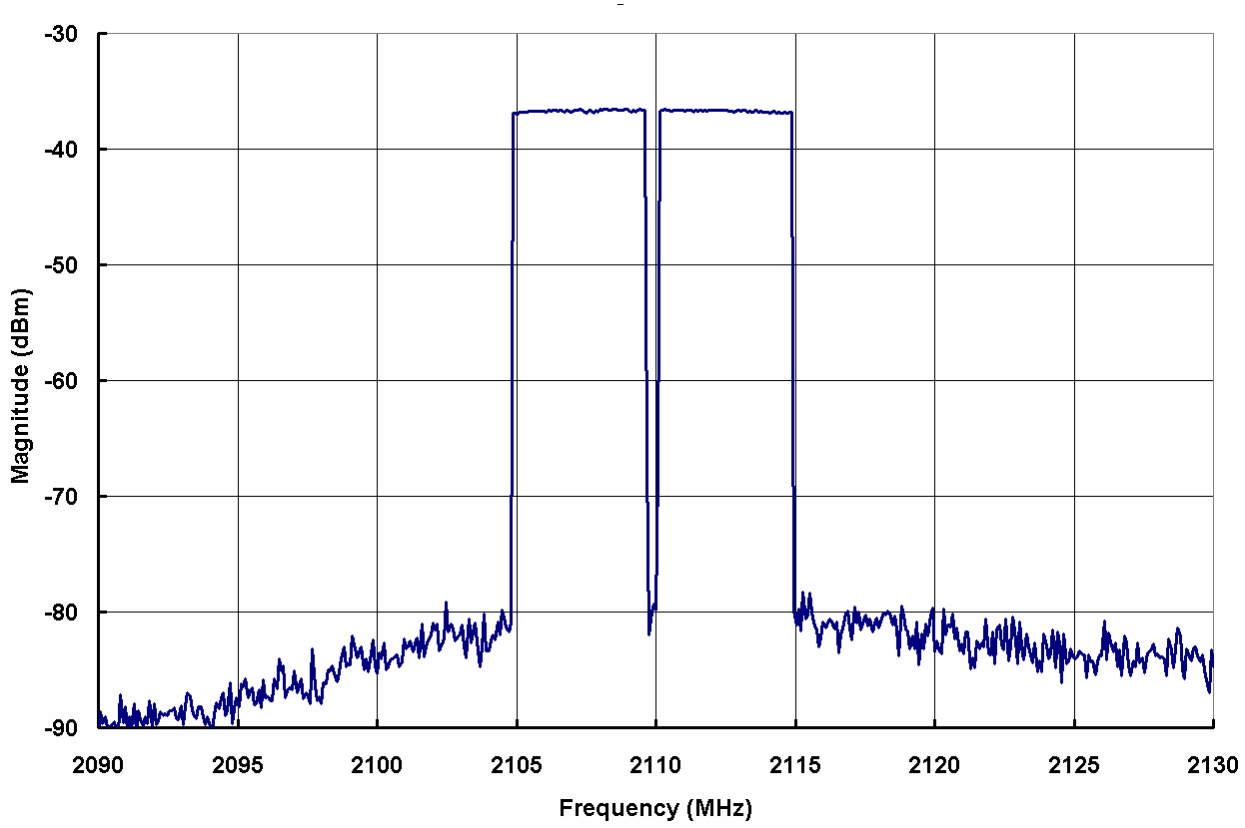

(a)

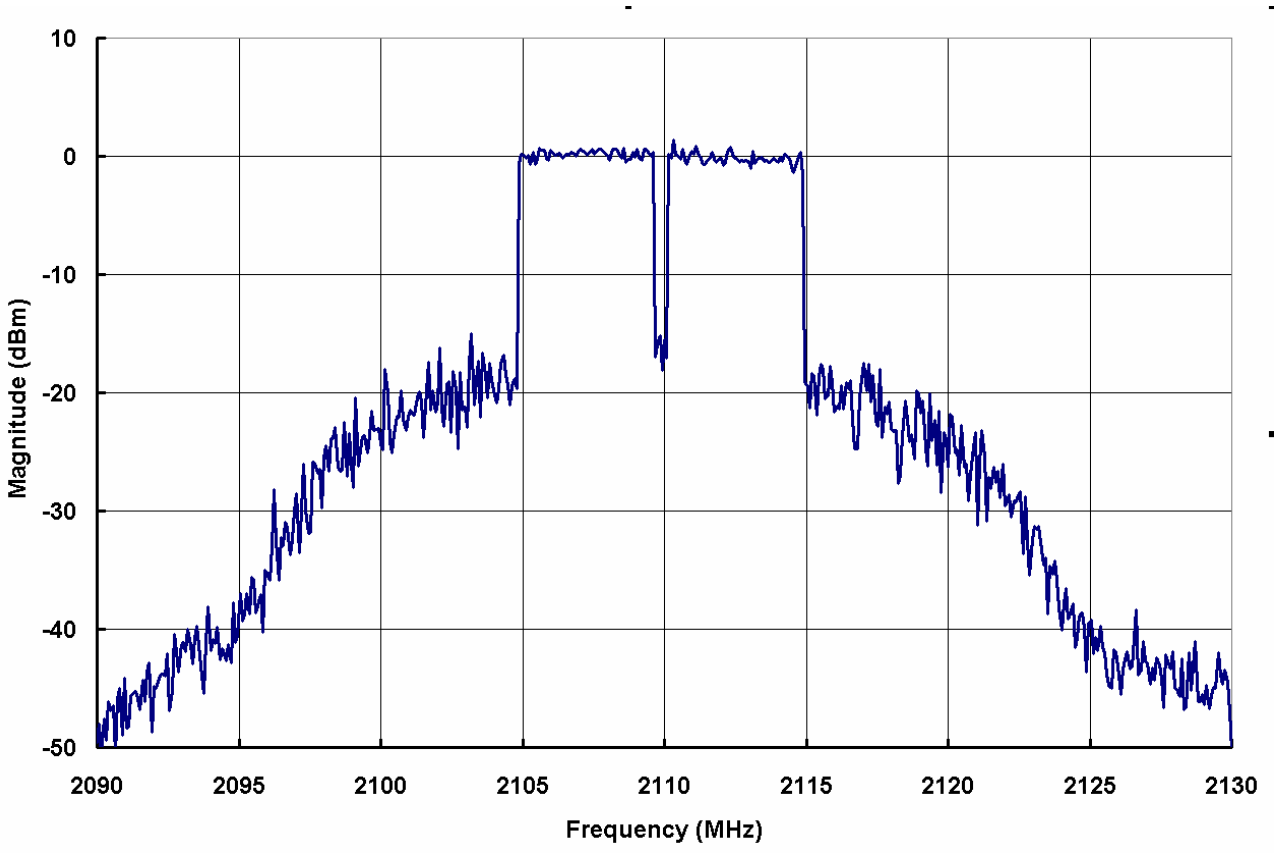

(b)

Fig. 13: (a) Input measured spectrum. (b) Output measured spectrum.
(a) Spectre d'entrée mesuré (b) Spectre de sortie mesuré

The designed notch is quasi ideal and then it is much more accurate than the one obtained using an analog NPR noise source technique and a notch filter. This is one of the main advantages offered by the use of a digital generation of stimuli.

NPR accuracy and variance versus the number of tones used to synthesized noise stimuli which has been theoretically investigated (figure 8) are experimentally verified here.
We have to generate a sufficient number of tones in order to decrease the NPR variance. Measurements have been done with 1000 and 10 000 tones to appreciate the effects of NPR variance.

The measurement procedure consists in recording the I and Q time domain waveforms with the digital oscilloscope at different input powers and phase draws. This waveform is a non-corrected complex envelope of the NPR response. Then, this envelope is corrected in the frequency domain with the calibration parameters : KI, KQ and $\Delta\phi$. Then we obtain a corrected spectrum corresponding to the RF modulated signal spectrum at the output of the amplifier under test. NPR is deduced from the power of each spectral line as explained in part II.

Figures 14 and 15 present NPR measurement results of a TI-HFET 1200 amplifier at 2,11 GHz obtained with a 20 MHz noise bandwidth and a 5% notch. Results are compared with those provided by an analog noise source measurement system. There are sketched 21 phase draws for 1000 tone (figure 14) and 10 000 tone (figure 15) stimuli.

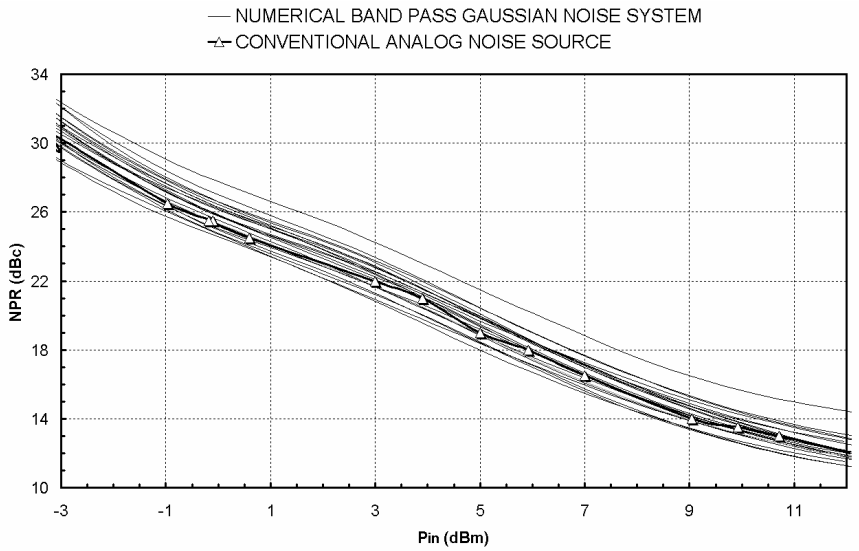

Fig. 14: Measurements using 21 different NPR stimuli with N=1000 and a 5% notch: output spectrum with 50 inter modulation lines into the notch.
Mesures en utilisant 21 stimuli différents avec N=1000 et un trou de 5%. Le spectre de sortie possède 50 raies d'intermodulation dans le trou

These measurements prove the validity of NPR results obtained by our new measurement approach. A 3 dB NPR peak to peak variation appears on curves in figure 14.
The same measurements realized with 10000 tones stimuli enable to reduce significantly the NPR variance. The final NPR curve is an average of all the measured curves. One notes that this final curve is very close to the result obtained with a conventional analog noise source setup.
We can conclude that our new measurement setup enables NPR characterization at L or S band by analyzing the time domain base band envelopes at the output of an amplifier under test. Moreover, this measurement setup has been easily extended to other frequency range like K or Ka bands.

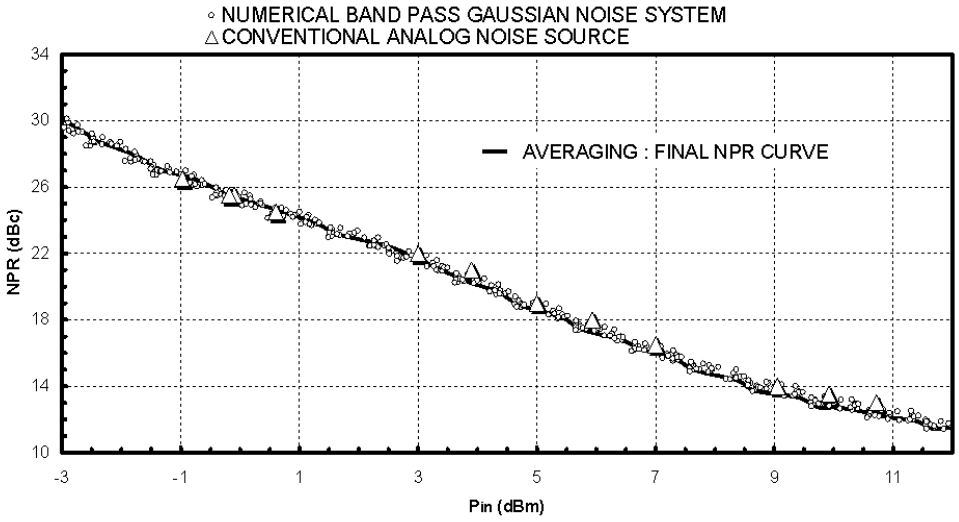

Fig. 15: Measurements using 21 different NPR stimuli with N=10000 and a 5% notch : output spectrum with 500 intermodulation lines into the notch.
Mesures en utilisant 21 stimuli différents avec N=10000 et un trou de 5%. Le spectre de sortie possède 500 raies d'intermodulation dans le trou

V. EXTENDED MEASUREMENTS AT KA BAND

An extension of this measurement system is easily realizable for NPR characterizations at other frequency bands. A configuration for Ka band measurements has been developed by using a second frequency translation [6]. The block diagram of this new configuration is represented in figure 16.

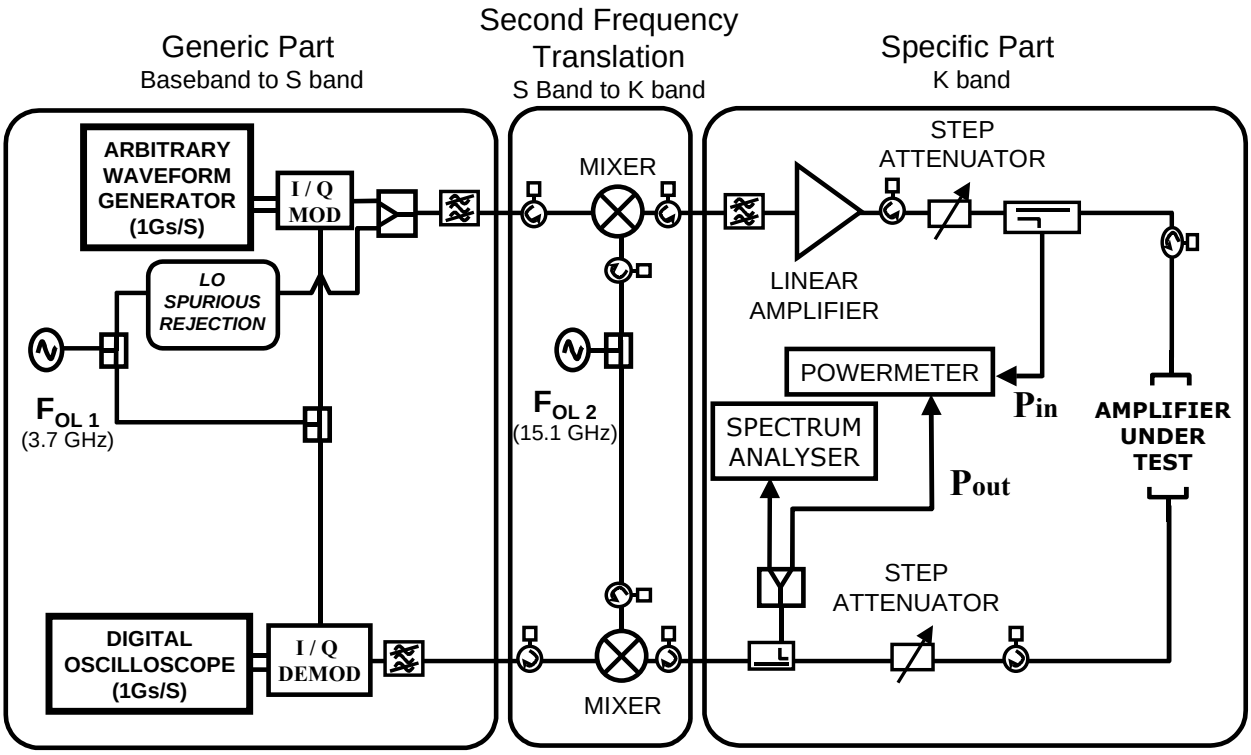

Fig. 16: Ka band measurement setup block diagram.
Synoptique du banc de mesure en bande Ka.

The generic part is the same as for L and S band measurements.
The local oscillator OL1 is fixed to 3,7GHz. The second local oscillator OL2 fixes the AUT characterization frequency.

This measurement setup configuration has been developed with a 1 Gs/s; 10 bits AWG and a 500 MHz, 8 bits sampling scope. The specific part depends on the OL2 frequency value.

Measurements of a 80 Watts traveling wave tube amplifier were performed at 19 GHz.
The spectrum measured at the output of the generic part (S band), and at the AUT input (Ka band) are presented in figure 17.

The digital generation of the pseudo-noise stimulus enables an accurate generation of the notch.

NPR results obtained with 10 stimuli composed of 25000 tones in a 250 MHz bandwidth and a 5% notch are given figure 18.

The NPR accuracy is around ±0.3 dB.

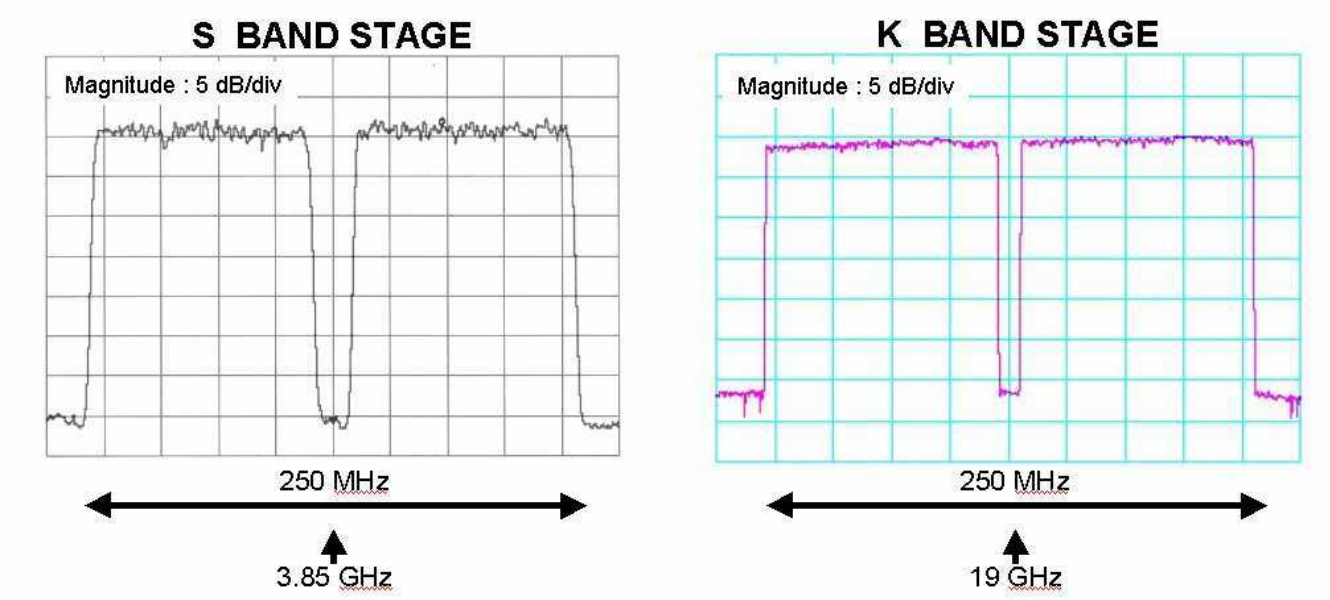

Fig. 17: Measured spectrum at the output of the generic part and at the input of the AUT.
Spectre mesuré en sortie de la partie générique et en entrée de l'amplificateur sous test.

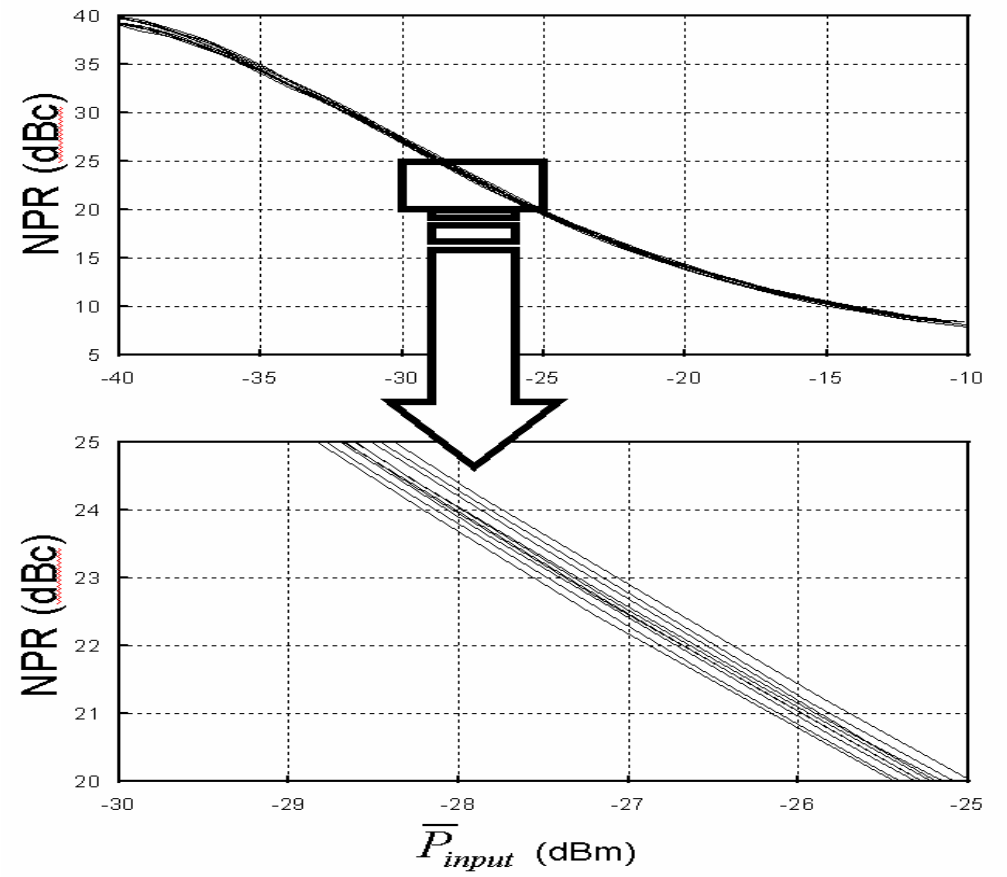

Fig. 18: Measurements of a T.W.T amplifier with 10 different phase draws.
Mesures d'un ATOP avec 10 tirages de phase différents.

VI. Conclusion

A new NPR characterization method based on a digital synthesis of pseudo noise stimuli and calibrated time domain measurement of complex envelopes has been presented. A major advantage of this method lies in the flexibility of the test signal conditioning. Furthermore, NPR measurements using this technique are not sensitive to the noise figure of the components of the system measurement because a FFT windowing and an averaging are performed on discrete spectral lines. This is not the case if the analog noise source technique is used.

The digital generation with a AWG enables NPR characterization with a very accurate defined notch and with a very good repeatability. The use of a limited number of tones for the NPR stimulus enables comparisons between measurements and harmonic balance or transient envelope simulations.

Furthermore, the calibrated measurement system is a very useful tool for the behavioral characterization and modeling of power amplifiers exhibiting nonlinear memory effects.

Acknowledgment

The authors would like to thank the French Space Agency (CNES) for their financial support, and F. Brasseau and O. Havard from Alcatel Space Industries (France) for NPR measurements using the analog white noise source technique.

References

[1] Westcott (R.J), Investigation of multiple f.m./f.d.m. carriers through a satellite t.w.t. operating near to saturation, *Proc. IEE*, vol. **114**, n°**6**, pp.726-740, june 1967

[2] Chen (S.W.), Panton (W.), Gilmore (R.), Effects of Nonlinear Distortion on CDMA Communication Systems, *IEEE Transactions on MTT*, vol. **44**, n°. **12**, pp 2743-2750, Dec. 1996

[3] Lajoinie (J.), Ngoya (E.), Barataud (D.), Nebus (J.M.), Sombrin (J.), Rivierre (B.), Efficient Simulation of NPR for the Optimum Design of Satellite Transponders SSPAs, *IEEE MTT-S Digest*, 1998, pp 775-778

[4] Rosen (H.A.), Owens (A.T.), Power Amplifier Linearity Studies for SSB Transmissions, *IEEE Transactions on Communications Systems*, vol. **12**, n°. 2, june 1964, pp.150-159

[5] Agilent, Noise power ratio (NPR) measurements using the HP, 2507B/E2508A multi-format communications signal simulator, *Application note* - literature number **5965-8533E**

[6] Pedro (J.C.), Carvalho (N.B.), A novel nonlinear distortion characterisation standard for RF and microwave communication systems, *Engineering science and education journal*, pp.113-119, june 2001.

[7] Mallet (A.), Gizard (F.), Reveyrand (T.), Lapierre (L.), Sombrin (J.), A new satelite repeater amplifier characterization system for large bandwith NPR and modulated signals measurements, *IEEE MTT-S International Microwave Symposium 2002*, Seattle, USA, June 2002

[8] Begue (M.M.), Testing new digital RF communication systems with smart stimulus and analysis, *The 1995 advanced test solutions for aerospace and defence seminar*, Hewlett-Packard

[9] Sombrin (J.), Critère de comparaison, d'optimisation et d'utilisation optimale des amplificateurs de puissance non-linéaires, *Rapport CNES*, Ref. **CNES DT-96-16-CT/AE/TTL/HY**, 24 mai 1996

[10] Reveyrand (T.), Barataud (D.), Lajoinie (J.), Campovecchio (M.), Nebus (J.-M.), Ngoya (E.), Sombrin (J.), Roques (D.), A Novel Experimental Noise Power Ratio Characterization Method for Multicarrier Microwave Power Amplifiers, *55th ARFTG Conference*, Boston, USA, June 2000